PHYSICAL REVIEW D **77,** 091101(R) (2008)

Measurement of the branching fraction and charge asymmetry of the decay $B^+ \to D^+ \bar{D}^0$ and search for $B^0 \to D^0 \bar{D}^0$

I. Adachi,[7] H. Aihara,[36] K. Arinstein,[1] V. Aulchenko,[1] T. Aushev,[11,16] A. M. Bakich,[33] V. Balagura,[11] K. Belous,[10] V. Bhardwaj,[28] U. Bitenc,[12] S. Blyth,[21] A. Bondar,[1] A. Bozek,[23] M. Bračko,[12,17] J. Brodzicka,[7] Y. Chao,[22] A. Chen,[20] K.-F. Chen,[22] W. T. Chen,[20] B. G. Cheon,[5] R. Chistov,[11] I.-S. Cho,[41] S.-K. Choi,[4] Y. Choi,[32] J. Dalseno,[7] M. Dash,[40] S. Eidelman,[1] D. Epifanov,[1] S. Fratina,[12] H. Ha,[14] J. Haba,[7] T. Hara,[27] M. Hazumi,[7] D. Heffernan,[27] Y. Hoshi,[35] W.-S. Hou,[22] H. J. Hyun,[15] K. Inami,[18] A. Ishikawa,[29] H. Ishino,[37] M. Iwasaki,[36] Y. Iwasaki,[7] D. H. Kah,[15] N. Katayama,[7] H. Kawai,[2] T. Kawasaki,[25] H. Kichimi,[7] H. J. Kim,[15] S. K. Kim,[31] K. Kinoshita,[3] S. Korpar,[12,17] P. Krokovny,[7] C. C. Kuo,[20] Y. Kuroki,[27] A. Kuzmin,[1] Y.-J. Kwon,[41] J. S. Lee,[32] M. J. Lee,[31] S. E. Lee,[31] T. Lesiak,[23] S.-W. Lin,[22] C. Liu,[30] D. Liventsev,[11] F. Mandl,[9] S. McOnie,[33] T. Medvedeva,[11] W. Mitaroff,[9] K. Miyabayashi,[19] H. Miyata,[25] Y. Miyazaki,[18] R. Mizuk,[11] D. Mohapatra,[40] M. Nakao,[7] Z. Natkaniec,[23] S. Nishida,[7] O. Nitoh,[39] S. Ogawa,[34] T. Ohshima,[18] S. Okuno,[13] P. Pakhlov,[11] G. Pakhlova,[11] C. W. Park,[32] H. Park,[15] H. K. Park,[15] L. S. Peak,[33] L. E. Piilonen,[40] A. Poluektov,[1] H. Sahoo,[6] Y. Sakai,[7] O. Schneider,[16] J. Schümann,[7] C. Schwanda,[9] K. Senyo,[18] M. Shapkin,[10] H. Shibuya,[34] J.-G. Shiu,[22] A. Somov,[3] M. Starič,[12] T. Sumiyoshi,[38] M. Tanaka,[7] Y. Teramoto,[26] K. Trabelsi,[7] T. Tsuboyama,[7] S. Uehara,[7] K. Ueno,[22] Y. Unno,[5] S. Uno,[7] Y. Usov,[1] G. Varner,[6] K. E. Varvell,[33] K. Vervink,[16] P. Wang,[8] Y. Watanabe,[13] E. Won,[14] Y. Yamashita,[24] C. C. Zhang,[8] Z. P. Zhang,[30] V. Zhilich,[1] V. Zhulanov,[1] A. Zupanc,[12] and O. Zyukova[1]

(Belle Collaboration)

[1]*Budker Institute of Nuclear Physics, Novosibirsk*
[2]*Chiba University, Chiba*
[3]*University of Cincinnati, Cincinnati, Ohio 45221*
[4]*Gyeongsang National University, Chinju*
[5]*Hanyang University, Seoul*
[6]*University of Hawaii, Honolulu, Hawaii 96822*
[7]*High Energy Accelerator Research Organization (KEK), Tsukuba*
[8]*Institute of High Energy Physics, Chinese Academy of Sciences, Beijing*
[9]*Institute of High Energy Physics, Vienna*
[10]*Institute of High Energy Physics, Protvino*
[11]*Institute for Theoretical and Experimental Physics, Moscow*
[12]*J. Stefan Institute, Ljubljana*
[13]*Kanagawa University, Yokohama*
[14]*Korea University, Seoul*
[15]*Kyungpook National University, Taegu*
[16]*École Polytechnique Fédérale de Lausanne (EPFL), Lausanne*
[17]*University of Maribor, Maribor*
[18]*Nagoya University, Nagoya*
[19]*Nara Women's University, Nara*
[20]*National Central University, Chung-li*
[21]*National United University, Miao Li*
[22]*Department of Physics, National Taiwan University, Taipei*
[23]*H. Niewodniczanski Institute of Nuclear Physics, Krakow*
[24]*Nippon Dental University, Niigata*
[25]*Niigata University, Niigata*
[26]*Osaka City University, Osaka*
[27]*Osaka University, Osaka*
[28]*Panjab University, Chandigarh*
[29]*Saga University, Saga*
[30]*University of Science and Technology of China, Hefei*
[31]*Seoul National University, Seoul*
[32]*Sungkyunkwan University, Suwon*
[33]*University of Sydney, Sydney, New South Wales*
[34]*Toho University, Funabashi*
[35]*Tohoku Gakuin University, Tagajo*
[36]*Department of Physics, University of Tokyo, Tokyo*
[37]*Tokyo Institute of Technology, Tokyo*

[38]*Tokyo Metropolitan University, Tokyo*
[39]*Tokyo University of Agriculture and Technology, Tokyo*
[40]*Virginia Polytechnic Institute and State University, Blacksburg, Virginia 24061*
[41]*Yonsei University, Seoul*
(Received 21 February 2008; published 7 May 2008)

We report an improved measurement of the $B^+ \to D^+\bar{D}^0$ and $B^0 \to D^0\bar{D}^0$ decays based on 657×10^6 $B\bar{B}$ events collected with the Belle detector at KEKB. We measure the branching fraction and charge asymmetry for the $B^+ \to D^+\bar{D}^0$ decay: $\mathcal{B}(B^+ \to D^+\bar{D}^0) = (3.85 \pm 0.31 \pm 0.38) \times 10^{-4}$ and $A_{CP}(B^+ \to D^+\bar{D}^0) = 0.00 \pm 0.08 \pm 0.02$, where the first error is statistical and the second is systematic. We also set the upper limit for the $B^0 \to D^0\bar{D}^0$ decay: $\mathcal{B}(B^0 \to D^0\bar{D}^0) < 0.43 \times 10^{-4}$ at 90% CL.

DOI: 10.1103/PhysRevD.77.091101 PACS numbers: 13.25.Hw, 14.40.Lb

Recently, evidence of direct CP violation in $B^0 \to D^+D^-$ decays was observed by the Belle collaboration [1], while *BABAR* measured an asymmetry consistent with zero [2]. A large direct CP asymmetry for this decay can indicate the presence of new-physics effects in the electroweak penguin sector [3]. A similar effect might be observable in the charged mode $B^+ \to D^+\bar{D}^0$. This decay has already been observed by Belle [4] and confirmed by *BABAR* [5]. The latter analysis also includes charge asymmetry measurement.

In this paper, we report an improved measurement of the branching fraction and charge asymmetry for $B^+ \to D^+\bar{D}^0$ decay and a search for the decay $B^0 \to D^0\bar{D}^0$. The latter can only be produced by a W exchange diagram. We use a data sample of $(657 \pm 9) \times 10^6$ $B\bar{B}$ events collected with the Belle detector at the KEKB collider [6]. The inclusion of charge-conjugate states is implicit throughout this paper.

The Belle detector is a large-solid-angle magnetic spectrometer that consists of a silicon vertex detector (SVD), a 50-layer central drift chamber (CDC), an array of aerogel threshold Cherenkov counters (ACC), a barrel-like arrangement of time-of-flight scintillation counters (TOF), and an electromagnetic calorimeter (ECL) comprised of CsI(Tl) crystals located inside a superconducting solenoid coil that provides a 1.5 T magnetic field. An iron flux-return located outside the coil is instrumented to detect K_L mesons and to identify muons (KLM). The detector is described in detail elsewhere [7]. For the first sample of 152×10^6 $B\bar{B}$ pairs, a 2.0 cm radius beam pipe and a 3-layer silicon vertex detector were used; for the latter 505×10^6 $B\bar{B}$ pairs, a 1.5 cm radius beam pipe, a 4-layer silicon detector and a small-cell inner drift chamber were used [8].

Each track's transverse momentum with respect to the beam axis is required to be greater than 0.075 GeV/c in order to reduce the combinatorial background. For charged particle identification (PID), the measurement of the specific ionization (dE/dx) in the CDC, and signals from the TOF and the ACC are used. Charged kaons are selected with PID criteria that have an efficiency of 88% with a pion misidentification probability of 8%. All charged tracks that are consistent with a pion hypothesis and that are not positively identified as electrons are treated as pion candidates.

Neutral kaons are reconstructed in the decay $K_S \to \pi^+\pi^-$; no PID requirements are applied for the daughter pions. The two-pion invariant mass is required to be within 9 MeV/c^2 ($\sim 3\sigma$) of the K^0 mass and the displacement of the $\pi^+\pi^-$ vertex from the interaction point (IP) in the transverse ($r - \varphi$) plane is required to be between 0.2 cm and 20 cm. The K_S momentum and the vector from the IP to the $\pi^+\pi^-$ vertex are required to be collinear in the $r - \varphi$ plane to within 0.2 radians.

Photon candidates are selected from ECL showers not associated with charged tracks. An energy deposition of at least 75 MeV and a photonlike shape of the shower are required for each candidate. A pair of photons with an invariant mass within 12 MeV/c^2 ($\sim 2.5\sigma$) of the π^0 mass is considered as a π^0 candidate. We require that the π^0 momentum be greater than 0.35 GeV/c in order to reduce the combinatorial background.

We reconstruct $\bar{D}^0$ mesons in the $K^+\pi^-$, $K^+\pi^-\pi^+\pi^-$, and $K^+\pi^-\pi^0$ decay channels. The D^+ candidates are reconstructed in the $K^-\pi^+\pi^+$ and $K_S\pi^+$ final states. We require the invariant mass of the $\bar{D}^0$ and D^+ candidates to be within 11 MeV/c^2 (1.5σ for $K^+\pi^-\pi^0$ and 2.5σ for other modes) of their nominal mass. We perform a mass-constrained fit for D candidates to improve their momentum resolution.

To suppress the large background from $B^+ \to D_s^+\bar{D}^0$ with the K^+ from the D_s^+ decay misidentified as a pion, none of the pions from D^+ should be consistent with the kaon hypothesis. This requirement has an efficiency of 93% and kaon misidentification probability of 9%.

We combine $\bar{D}^0$ and D^+ (D^0) candidates to form B^+ (B^0) candidates. These are identified by their center-of-mass (CM) energy difference, $\Delta E = (\sum_i E_i) - E_{\rm beam}$, and the beam constrained mass, $M_{\rm bc} = \sqrt{E_{\rm beam}^2 - (\sum_i \vec{p}_i)^2}$, where $E_{\rm beam}$ is the beam energy and $\vec{p}_i$ and E_i are the momenta and energies of the decay products of the B meson in the CM frame. We select events with $M_{\rm bc} > 5.2$ GeV/c^2 and $|\Delta E| < 0.3$ GeV, and define a B signal region of $|\Delta E| < 0.02$ GeV, 5.273 GeV/$c^2 < M_{\rm bc} < 5.287$ GeV/c^2. In an event with more than one B candidate, we choose the one with smallest χ^2 from the D mass-constrained fit. We use Monte Carlo (MC) simulation to

model the response of the detector and determine the efficiency [9].

Variables that characterize the event topology are used to suppress background from the jetlike $e^+e^- \to q\bar{q}$ continuum process. We require $|\cos\theta_{\rm thr}| < 0.8$, where $\theta_{\rm thr}$ is the angle between the thrust axis of the B candidate and that of the rest of the event; this condition rejects 77% of the continuum background while retaining 78% of the signal. To suppress high background in the $D^0\bar{D}^0$ final state, we use a Fisher discriminant, $\mathcal{F}$, that is based on the production angle of the B candidate, the angle of the B candidate thrust axis with respect to the beam axis, and nine parameters that characterize the momentum flow in the event relative to the B candidate thrust axis in the CM frame [10]. We impose a requirement on $\mathcal{F}$ that rejects 52% of the remaining continuum background and retains 86% of the signal.

We determine the signal yield from the two-dimensional unbinned extended maximum likelihood fit (2D) to the ΔE- $M_{\rm bc}$ distribution. The signal probability density function (PDF) is described by a double Gaussian for ΔE and a single Gaussian for $M_{\rm bc}$, taking into account ΔE- $M_{\rm bc}$ correlations. We use the $B^+ \to D_s^+\bar{D}^0$ events in our data sample to calibrate the means and resolutions of the signal shape. The continuum, $B\bar{B}$ and $B^+ \to D_s^+\bar{D}^0$ background contributions are described separately. We use a linear function for ΔE and a threshold function for $M_{\rm bc}$ [11] to describe the continuum PDF. The $B\bar{B}$ background is modeled by a quadratic polynomial for ΔE, a threshold function for $M_{\rm bc}$ combined with a small peaking component (a wide Gaussian for ΔE and a Gaussian for $M_{\rm bc}$). The shape of the peaking background and parameters of the threshold function are fixed from the generic $B\bar{B}$ MC. The ΔE linear slope and quadratic term are free parameters. The peak in the ΔE distribution near -70 MeV coming from the $B^+ \to D_s^+\bar{D}^0$ decay is described by a Gaussian for ΔE and a Gaussian for $M_{\rm bc}$. Again, we use $B^+ \to D_s^+\bar{D}^0$ to obtain the parameters of this PDF. The region $\Delta E < -0.1$ GeV is excluded from the fit to avoid contributions from $B \to \bar{D}D^*$ decays.

As a cross-check, we also perform separate one-dimensional fits to the ΔE and $M_{\rm bc}$ distributions, requiring the other variable to be in the signal region. The results are given in Table I, where the listed efficiencies include intermediate branching fractions. The projections of the 2D fit result are shown in Figs. 1 and 2. The 90% confidence level (CL) upper limit for $B^0 \to D^0\bar{D}^0$ signal yield is obtained using the POLE program [12] based on the Feldman-Cousins method [13]. The systematic uncertainty (described later) is taken into account in this calculation.

To calculate the charge asymmetry in the $B^+ \to D^+\bar{D}^0$ decay channel, we repeat the fits separately for the $B^+ \to D^+\bar{D}^0$ and $B^- \to D^-D^0$ samples. The ΔE distributions for $B^+ \to D^+\bar{D}^0$ and $B^- \to D^-D^0$ candidates are presented in Fig. 3. The fit results are given in Table II. Using the results of the 2D fits, we obtain the charge asymmetry:

TABLE I. Yields from the ΔE, $M_{\rm bc}$ and 2D (ΔE- $M_{\rm bc}$) fits, detection efficiencies including intermediate branching fractions, and corresponding branching fractions. Upper limits are at the 90% CL.

Decay channel	ΔE yield	$M_{\rm bc}$ yield	2D yield	ε, 10^{-4}	$\mathcal{B}$, 10^{-4}
$B^0 \to D^0\bar{D}^0$	-4.5 ± 29.7	5.7 ± 28.6	0.4 ± 24.8 (< 46)	16.4	<0.43
$B^\pm \to D^\pm D^0$	366.4 ± 31.8	376.4 ± 30.7	369.7 ± 29.4	14.6	$3.85 \pm 0.31 \pm 0.38$

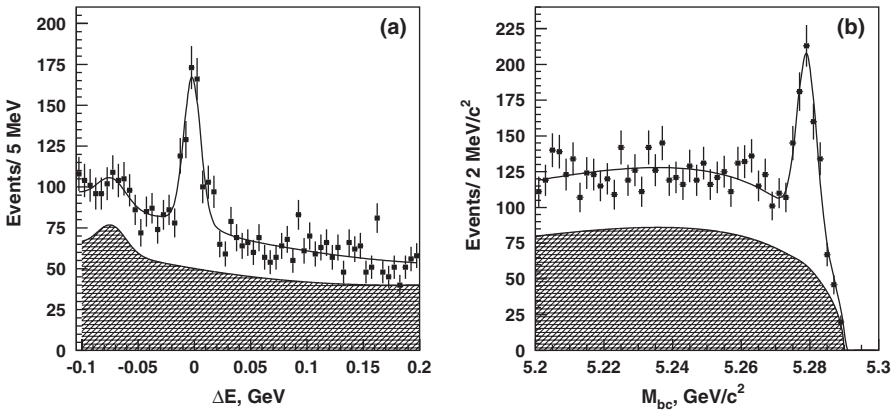

FIG. 1. ΔE (a) and $M_{\rm bc}$ (b) distributions for the $B^+ \to D^+\bar{D}^0$ candidates. Each distribution is the projection of the signal region of the other parameter. Points with errors represent the experimental data, open curves show projections from the 2D fits and crosshatched curves show the $B\bar{B}$ component only.

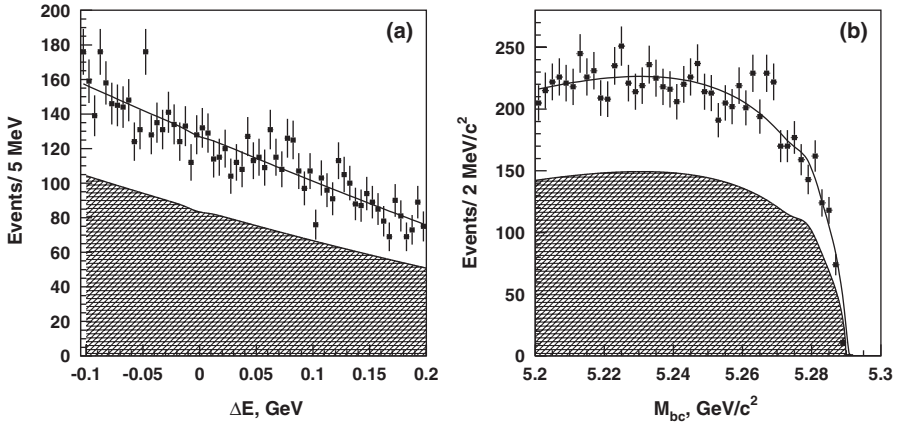

FIG. 2. ΔE (a) and $M_{\rm bc}$ (b) distributions for the $B^0 \to D^0\bar{D}^0$ candidates. Each distribution is the projection of the signal region of the other parameter. Points with errors represent the experimental data, open curves show projections from the 2D fits and crosshatched curves show the $B\bar{B}$ component only.

$$A_{CP} = \frac{N(D^-D^0) - N(D^+\bar{D}^0)}{N(D^-D^0) + N(D^+\bar{D}^0)} = 0.00 \pm 0.08 \pm 0.02.$$

We calculate the $B^+ \to D^+\bar{D}^0$ branching fraction separately for each D decay channel; the results are consistent with each other. As an additional check, we apply a similar procedure to a decay chain with a similar final state: $B^+ \to D_s^+\bar{D}^0$. We measure the branching fraction $\mathcal{B}(B^+ \to D_s^+\bar{D}^0) = (9.5 \pm 0.2) \times 10^{-3}$, where the error is statistical only. This is consistent with the world average value $(10.0 \pm 1.7) \times 10^{-3}$ [14]. The charge asymmetry in this final state is consistent with zero: $(-0.5 \pm 1.5)\%$. We also measure the charge asymmetry for the $D^+\bar{D}^0$ background events and find a value consistent with zero: $(-1.4 \pm 1.3)\%$.

Table III shows the sources of the systematic uncertainty. The errors due to knowledge of D branching fractions are taken from Ref. [14]. The uncertainty in the tracking efficiency is estimated using partially reconstructed $D^{*+} \to D^0[K_S\pi^+\pi^-]\pi^+$ decays. The uncertainty in the PID efficiency is determined from $D^{*+} \to D^0[K^-\pi^+]\pi^+$ decays. The error in signal yield determination is estimated by varying the signal and background shapes and fit range. We assume equal production rates for B^+B^- and $B^0\bar{B}^0$ pairs and do not include the uncertainty related to this assumption in the total systematic error.

The asymmetry measurement contains the following systematic errors: tracking efficiency difference for $\pi^\pm$ (0.013), particle identification efficiency difference for $\pi^\pm$ and $K^\pm$ (0.004) and signal yield determination (0.015). The total systematic uncertainty is 0.02.

In summary, we report improved measurements of the $B^+ \to D^+\bar{D}^0$ branching fraction $\mathcal{B}(B^+ \to D^+\bar{D}^0) = (3.85 \pm 0.31 \pm 0.38) \times 10^{-4}$. The charge asymmetry for this decay is measured to be consistent with zero $A_{CP}(B^+ \to D^+\bar{D}^0) = 0.00 \pm 0.08 \pm 0.02$. We also set an upper limit for the $B^0 \to D^0\bar{D}^0$ decay branching fraction of $\mathcal{B}(B^0 \to D^0\bar{D}^0) < 0.43 \times 10^{-4}$ at 90% CL. These results

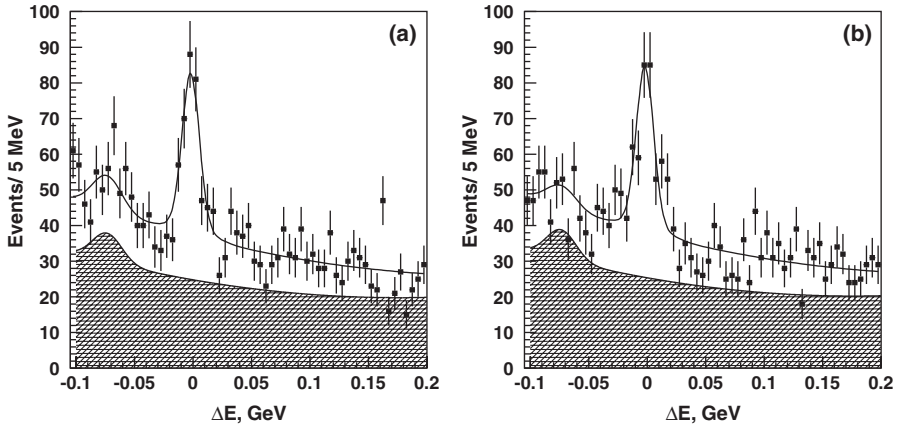

FIG. 3. The ΔE distribution for (a) $B^+ \to D^+\bar{D}^0$ and (b) $B^- \to D^-D^0$. Points with errors represent the experimental data, open curves show projections from the 2D fits and crosshatched curves show the $B\bar{B}$ component only.

TABLE II. Charged B meson yields from the ΔE, $M_{\rm bc}$ and 2D (ΔE- $M_{\rm bc}$) fits. Errors are statistical only.

Decay channel	ΔE yield	$M_{\rm bc}$ yield	2D yield
$B^+ \to D^+ \bar{D}^0$	183.9 ± 21.5	184.4 ± 21.4	184.2 ± 20.4
$B^- \to D^- D^0$	183.4 ± 22.1	192.5 ± 21.8	185.4 ± 21.0

are consistent with our previous results [4] and supersede them. Our results are also consistent with *BABAR* measurements [5].

We thank the KEKB group for the excellent operation of the accelerator, the KEK cryogenics group for the efficient operation of the solenoid, and the KEK computer group and the National Institute of Informatics for valuable computing and Super-SINET network support. We acknowledge support from the Ministry of Education, Culture, Sports, Science, and Technology of Japan and the Japan Society for the Promotion of Science; the Australian Research Council and the Australian Department of Education, Science and Training; the National Science Foundation of China and the Knowledge Innovation Program of the Chinese Academy of Sciences under contract No. 10575109 and IHEP-U-503; the Department of Science and Technology of India; the BK21 program of the Ministry of Education of Korea, the CHEP SRC program and Basic Research program (grant No. R01-2005-000-10089-0) of the Korea Science and Engineering Foundation, and the Pure Basic Research Group program of the Korea Research Foundation; the Polish State Committee for Scientific Research; the Ministry of Education and Science of the Russian Federation and the Russian Federal Agency for Atomic Energy; the Slovenian Research Agency; the Swiss National Science Foundation; the National Science Council and the Ministry of Education of Taiwan; and the U.S. Department of Energy.

TABLE III. Sources of systematic uncertainty.

Source	$\mathcal{B}(D^0\bar{D}^0)$	$\mathcal{B}(D^+\bar{D}^0)$	$A_{CP}(D^+\bar{D}^0)$
D branching fraction	7%	5%	0
Tracking	6%	6%	0.013
PID	2%	4%	0.004
π^0 reconstruction	2%	1.3%	0
$N(B\bar{B})$	1.4%	1.4%	0
MC statistics	1%	1%	0
Signal fit	4%	4%	0.015
Total	10.5%	9.8%	0.02

[1] S. Fratina *et al.* (Belle Collaboration), Phys. Rev. Lett. **98**, 221802 (2007).
[2] R. Aubert *et al.* (*BABAR* Collaboration), Phys. Rev. Lett. **99**, 071801 (2007).
[3] R. Fleisher, Eur. Phys. J. C **51**, 849 (2007).
[4] G. Majumder *et al.* (Belle Collaboration), Phys. Rev. Lett. **95**, 041803 (2005).
[5] R. Aubert *et al.* (*BABAR* Collaboration), Phys. Rev. D **73**, 112004 (2006).
[6] S. Kurokawa and E. Kikutani, Nucl. Instrum. Methods Phys. Res., Sect. A **499**, 1 (2003), and other papers therein.
[7] A. Abashian *et al.* (Belle Collaboration), Nucl. Instrum. Methods Phys. Res., Sect. A **479**, 117 (2002).
[8] Z. Natkaniec *et al.* (Belle SVD2 Group), Nucl. Instrum. Methods Phys. Res., Sect. A **560**, 1 (2006).
[9] R. Brun *et al.*, GEANT 3.21, Report No. CERN DD/EE/84-1, 1984.
[10] D. M. Asner *et al.* (CLEO Collaboration), Phys. Rev. D **53**, 1039 (1996).
[11] H. Albrecht *et al.* (ARGUS Collaboration), Phys. Lett. B **241**, 278 (1990).
[12] J. Conrad *et al.*, Phys. Rev. D **67**, 012002 (2003).
[13] G. J. Feldman and R. D. Cousins, Phys. Rev. D **57**, 3873 (1998).
[14] W.-M. Yao *et al.* (Particle Data Group), J. Phys. G **33**, 1 (2006), and partial update for 2007.